Nck adaptor proteins link Tks5 to invadopodia actin regulation and ECM degradation

Stanley S. Stylli[1], Stacey T. T. I[1], Anne M. Verhagen[2], San San Xu[1], Ian Pass[3], Sara A. Courtneidge[3] and Peter Lock[1,*,‡]

[1]Department of Surgery, University of Melbourne, Level 5, Clinical Sciences Building, Royal Melbourne Hospital, Parkville, Victoria 3052, Australia
[2]Walter and Eliza Hall Institute of Medical Research, Parkville, Victoria 3052, Australia
[3]Burnham Institute for Medical Research, Torrey Pines Road, La Jolla, CA 92037, USA

*Present address: Biochemistry Department, La Trobe University, Victoria 3086, Australia
‡Author for correspondence (e-mail: peteralanlock@gmail.com)

Accepted 5 May 2009
Journal of Cell Science 122, 2727-2740 Published by The Company of Biologists 2009
doi:10.1242/jcs.046680

Summary

Invadopodia are actin-based projections enriched with proteases, which invasive cancer cells use to degrade the extracellular matrix (ECM). The Phox homology (PX)-Src homology (SH)3 domain adaptor protein Tks5 (also known as SH3PXD2A) cooperates with Src tyrosine kinase to promote invadopodia formation but the underlying pathway is not clear. Here we show that Src phosphorylates Tks5 at Y557, inducing it to associate directly with the SH3-SH2 domain adaptor proteins Nck1 and Nck2 in invadopodia. Tks5 mutants unable to bind Nck show reduced matrix degradation-promoting activity and recruit actin to invadopodia inefficiently. Conversely, Src- and Tks5-driven matrix proteolysis and actin assembly in invadopodia are enhanced by Nck1 or Nck2 overexpression and inhibited by Nck1 depletion. We show that clustering at the plasma membrane of the Tks5 inter-SH3 region containing Y557 triggers phosphorylation at this site, facilitating Nck recruitment and F-actin assembly. These results identify a Src-Tks5-Nck pathway in ECM-degrading invadopodia that shows parallels with pathways linking several mammalian and pathogen-derived proteins to local actin regulation.

Supplementary material available online at
http://jcs.biologists.org/cgi/content/full/122/15/2727/DC1

Key words: Invadopodia, Podosome, Src, Tks5, Nck, ECM degradation

Introduction

Invasion and metastasis are hallmarks of tumour progression and the major cause of cancer mortality, but the underlying mechanisms of these devastating processes are complex and poorly understood. Minimally, for a tumour to disseminate, malignant cells must detach from the primary lesion, acquire a motile phenotype and penetrate the ECM of basement membranes and stroma which physically separate the tumour from the circulation (Condeelis and Segall, 2003; Friedl and Wolf, 2003). Depending on matrix density, tumour cells may exploit proteolytic and non-proteolytic mechanisms to breach ECM barriers (Friedl and Wolf, 2003; Friedl and Wolf, 2008). Destruction of ECM components is facilitated by secreted and membrane-bound extracellular proteases, including matrix metalloproteases (MMPs) and serine proteases acting independently or in proteolytic cascades (Basbaum and Werb, 1996; Linder, 2007).

In many tumour cells, enzymes responsible for matrix degradation are targeted to dynamic F-actin-enriched structures termed invadopodia, which are closely related molecularly and functionally to ventral adhesive structures called podosomes that are formed by several normal cell types (e.g. osteoclasts) as well as Src-transformed fibroblasts (Weaver, 2006; Linder, 2007; Gimona et al., 2008). Formation of invadopodia is enhanced by matrix rigidity (Alexander et al., 2008), some growth factors (Tague et al., 2004; Yamaguchi et al., 2005) or expression of wild-type or activated forms of Src tyrosine kinase (Chen et al., 1984; Artym et al., 2006). Numerous proteins and a subset of phosphoinositides are recruited to invadopodia and have roles in processes such as ECM degradation and adhesion, signal transduction, actin network assembly and membrane remodelling (Artym et al., 2006; Weaver, 2006; Linder, 2007). Extensive molecular cross-talk in invadopodia is suggested by the fact that depletion, inhibition or sequestration of individual constituents is usually sufficient to abrogate invadopodia formation (Bowden et al., 1999; Baldassarre et al., 2003; Chuang et al., 2004; Hashimoto et al., 2004; Tague et al., 2004; Onodera et al., 2005; Seals et al., 2005; Yamaguchi et al., 2005; Artym et al., 2006; Clark et al., 2007; Oikawa et al., 2008). Consistent with this, several physical interactions between invadopodia-localized proteins are critical for invadopodia function, such as those involving cortactin and AMAP1 (also known as ASAP1) (Onodera et al., 2005) and N-WASP and WIP (Yamaguchi et al., 2005) among others. Live cell studies also show that invadopodia assemble sequentially. For example, recruitment of cortactin precedes and is necessary for membrane type 1(MT1)-MMP accumulation at invadopodia and ensuing matrix degradation (Artym et al., 2006; Clark et al., 2007).

Several Src substrates are phosphorylated in invadopodia including cortactin (Ayala et al., 2008), AMAP1 (Bharti et al., 2007), paxillin (Badowski et al., 2008) and p130Cas (Alexander et al., 2008). Moreover, tyrosine phosphorylation of some of these proteins appears to be critical for their functional activity in regulating invadopodia and/or podosome dynamics and organization. Tks5 (also known as SH3PXD2A; formerly FISH) is a large adaptor molecule containing a phox homology (PX) and five SH3 domains (Lock et al., 1998). Although Tks5 was identified as a Src substrate and is highly phosphorylated in Src-transformed cells, the significance of Tks5 phosphorylation is unknown. Tks5 localizes in and its expression is critical for podosome formation as well as

the invasive potential of Src-transformed cells and several human tumour cell lines (Abram et al., 2003; Seals et al., 2005). Recruitment of Tks5 to podosomes is facilitated by the PX domain, which binds the phosphoinositides, PtdIns(3)*P* and PtdIns(3,4)P_2 in vitro (Abram et al., 2003; Oikawa et al., 2008). In keeping with this, PtdIns(3,4)P_2 accumulates in the early phases of podosome formation, in a Src-, PI 3-kinase- and synaptojanin-2-dependent manner, preceding Tks5 recruitment and actin assembly (Oikawa et al., 2008; Symons, 2008). Consistent with a role as an adaptor protein Tks5 can interact with multiple proteins found in podosomes including ADAM-family metalloproteases (Abram et al., 2003), the adhesion receptor, dystroglycan (Thompson et al., 2008), the SH3/SH2 adaptor, Grb2 and the nucleation promoting factor, N-WASP (Oikawa et al., 2008). Although it is not clear if these interactions occur simultaneously or sequentially or via direct or indirect associations, collectively these results suggest that Tks5 has a central role in invadopodia and podosome regulation. Here, we explored the mechanism by which Tks5 facilitates invadopodia formation in tumour cells.

Results

Tks5 synergises with Src to promote invadopodia and matrix proteolysis

A clear functional link between Src and Tks5 in podosome and invadopodia regulation has been demonstrated (Seals et al., 2005; Oikawa et al., 2008) but the extent to which these proteins cooperate to stimulate ECM degradation has not been quantified. To examine this, we first compared the abilities of metastatic B16F10 melanoma cells transiently expressing wild-type or activated Src (Src and Src Y527F) and/or FLAG-epitope-tagged Tks5 to degrade matrices of FITC-labelled gelatin during a 24-hour period. B16F10 cells were selected for this analysis because they express relatively high levels of endogenous Tks5, form robust invadopodia enriched with both Tks5 and F-actin (supplementary material Fig. S1A,B) and exhibit a reproducibly high transfection efficiency (40-60%, based on GFP marker studies; data not shown). In the 24-hour matrix degradation assay used, the area of cleared gelatin, normalized for cell number, was determined in multiple independent microscope fields. Values are expressed as mean degradation area (μm^2)/cell and provide a measure of the average matrix degradation activity of a cell in the sample population, irrespective of transfection status, cell movements or individual activities of cells during the assay. Zones of gelatin degradation are therefore not assigned to specific cells as in some other assays. The average levels of transiently expressed and endogenous proteins are assessed in parallel by immunoblot analysis.

As shown in Fig. 1A-C, the basal matrix degradation activity of the parental B16F10 cells was not affected by transfection with an empty vector but was boosted approximately three- and fivefold in cells expressing Src and Src Y527F, respectively. Expression of N- or C-terminal FLAG-Tks5 alone also resulted in significant (sixfold) enhancement of matrix degradation, whereas coexpression of Tks5 proteins in the presence of wild-type or active Src, resulted in super-additive increases in matrix degradation (up to 15- and 17-fold, respectively). We observed a similar functional cooperativity between Src and Tks5 in MDA-MB-231 breast carcinoma cells (supplementary material Fig. S1C,D). Expression of Src or Src Y527F in these cells has been reported to enhance invadopodia formation and overall matrix degradation (Artym et al., 2006). In our hands, expression of Src Y527F and, to a greater extent, N-FLAG-Tks5, enhanced the basal matrix degradation activity of MDA-MB-231 cells, whereas coexpression of Src Y527F and Tks5 produced a synergistic increase in matrix degradation.

The effect of reduced Tks5 expression on matrix degradation was also tested in parental and Src Y527F-expressing B16F10 cells using RNAi. Endogenous Tks5 levels were strongly suppressed by Tks5 siRNA treatment and coinciding with this, basal and Src-induced gelatin degradation was markedly diminished (supplementary material Fig. S1E,F). These results support earlier work showing that Tks5 is needed for podosome formation and matrix degradation in Src-transformed fibroblasts and tumour cells (Seals et al., 2005).

To confirm that the effects of altered Tks5 levels on Src-driven matrix degradation are related to invadopodia formation, we used a 4-hour matrix degradation assay to compare the functional activity and subcellular localization of a full-length Tks5-GFP fusion protein versus GFP in Src Y527F-expressing B16F10 cells. Unlike the 24-hour matrix degradation assay, only degradation associated with individual GFP-positive cells was analysed. Whereas Tks5-GFP colocalized extensively with Src in invadopodia of the Src Y527F-expressing cells, GFP was distributed throughout the nucleus and cytoplasm of cells and not recruited to invadopodia (Fig. 1E). Correlating with Tks5-GFP recruitment to invadopodia and confirming its biological activity, Tks5-GFP expression significantly enhanced the matrix degradation activity of cells compared with GFP alone (Fig. 1F).

Identification of Nck1/2 in association with Tks5

We postulated that Tks5 is dependent on interactions with cellular target proteins for its activity and that such interactions may be Src dependent. The isolated SH3 and PX domains of Tks5 have been used previously as affinity reagents to identify Tks5-interacting proteins (Abram et al., 2003; Seals et al., 2005; Oikawa et al., 2008). However, a potential disadvantage of this approach is that it excludes the 'linker' regions between the PX and SH3 domains (supplementary material Fig. S2A), which contain numerous polyproline motifs and suspected phosphorylation sites that could potentially interface with other proteins (Lock et al., 1998). To identify proteins in association with intact Tks5, full length N- and C-FLAG-Tks5 were coexpressed with Src in 60×15 cm dishes of 293T cells (supplementary material Fig. S2A). A Tks5 variant lacking the PX domain, FLAG-ΔPX-Tks5, was also included, based on evidence that the PX domain interferes with SH3 domain binding (Abram et al., 2003). 293T cells lack endogenous Tks5 as assessed by immunoblot analysis (not shown). FLAG-Tks5 complexes were purified from cell lysates by binding to immobilized FLAG antibody, then eluted with a FLAG peptide, resolved by SDS-PAGE and stained with Sypro Ruby (supplementary material Fig. S2B) and proteins identified by mass spectrometry (supplementary material Table S1).

A number of candidate proteins with known or potential roles in invadopodia, actin regulation or tyrosine kinase signalling appeared to associate specifically with Tks5 (supplementary material Table S1) but not with Tks5-unrelated FLAG-tagged proteins screened separately (A.M.V., unpublished data). Among them, were cortactin, Nck1, Nck2, Grb2, CrkL, drebrin and SH3P7. In co-immunoprecipitation assays designed to validate some of these interactions, however, we could not confirm a stable interaction of Tks5 with cortactin, CrkL (Fig. 2A) or SH3P7 (data not shown). The reasons for this are unclear but may be related to the high sensitivity of the mass spectrometry versus the relatively high stringency of the co-immunoprecipitation assay. We note that Grb2

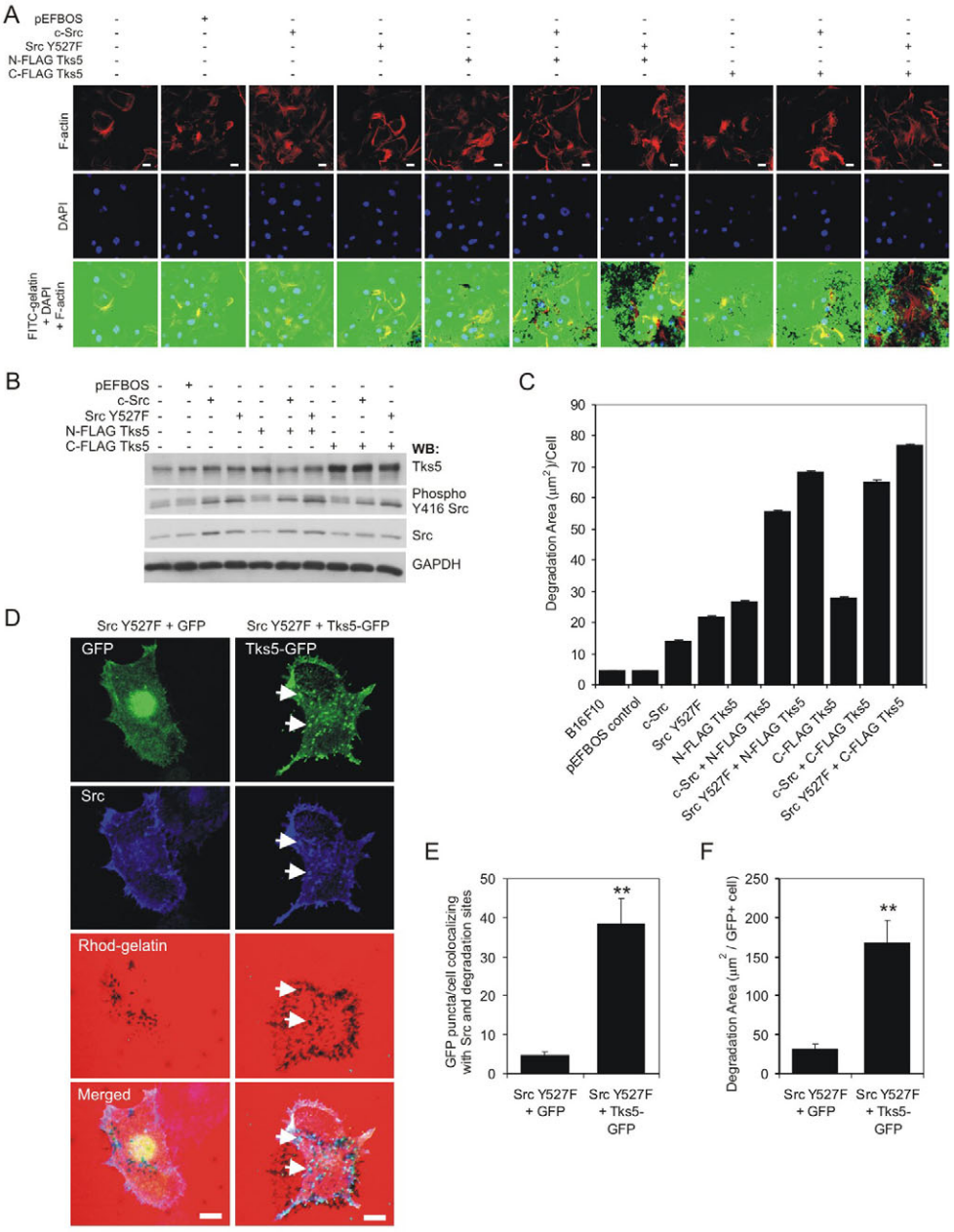

Fig. 1. Src and Tks5 induce invadopodia synergistically. (A) Representative confocal microscopy images showing strong induction of degradation (black areas in bottom row) of FITC-gelatin films (green) by co-transfection of B16F10 melanoma cells with Src and Tks5. F-actin (red) and nuclei (blue) were stained with TRITC-phalloidin and DAPI, respectively. pEFBOS, control vector. Scale bars: 20 μm. (B) Immunoblot showing Tks5, Src and active (Y416-*P*)-Src expression levels in B16F10 cells transiently transfected with the indicated constructs (corresponds to groups shown in A). (C) Quantification of the average matrix degradation activity of the indicated B16F10 transfectants reveals that Src and Tks5 promote matrix degradation cooperatively. Graph shows the mean degradation area/cell + s.e.m. n=41 fields (>600 cells total)/group, three experiments; P<0.01 for all pairwise comparisons except B16F10 versus pEFBOS and N- versus C-FLAG-Tks5. (D) Confocal images showing examples of single B16F10 cells coexpressing Src Y527F (blue) and GFP or Tks5-GFP (green) 4 hours after seeding on Rhodamine-gelatin (red). Arrows indicate colocalization of Src and Tks5-GFP in invadopodia. Scale bars: 10 μm. (E,F) Quantification of (E) the GFP puncta colocalizing with Src and (F) matrix degradation reveals significant Tks5-GFP recruitment to Src-containing invadopodia and enhanced matrix degradation. Columns and error bars represent means + s.e.m. (n=10 cells/group). **P<0.01 for indicated comparisons.

was identified as a Tks5-binding protein recently (Oikawa et al., 2008).

In contrast to the other candidate proteins tested we found that endogenous Nck co-immunoprecipitated readily with each of the FLAG-Tks5 bait proteins (Fig. 2A,D), associating preferentially with Tks5 isolated from Src-expressing cells and correlating with increased Tks5 tyrosine phosphorylation. We also noticed that the PX domain of Tks5 appears to be inhibitory for Nck binding: significantly more Nck co-immunoprecipitated with FLAG-ΔPX-Tks5 than with either N-FLAG-Tks5 (Fig. 2A,B) or C-FLAG-Tks5 (not shown). The p47phox adaptor protein is a cytosolic subunit of the NADPH oxidase complex which shares a similar architecture (PX-SH3-SH3) and significant homology with the N-terminal PX domain and first two SH3 domains of Tks5 (Lock et al., 1998). Structural and biochemical studies have suggested that the second SH3 domain of p47phox, either alone or in tandem with the first SH3 domain, can interact intramolecularly with proline-containing motifs in the p47phox PX domain or C-terminus, respectively, and thereby promote an auto-inhibited conformation (Karathanassis et al., 2002; Ago et al., 2003; Groemping et al., 2003). On this basis we examined the role of the second Tks5 SH3 domain in Nck binding to Tks5. Inactivation of the SH3 domain by the substitution, W260R (Karathanassis et al., 2002), resulted in increased co-immunoprecipitation of Nck with N-FLAG-Tks5 to levels similar to those of FLAG-ΔPX-Tks5 (Fig. 2A). Quantification of Nck and phosphotyrosine immunoblots in two independent experiments revealed that the increased binding of Nck to both ΔPX-Tks5 and the full-length W260R mutant relative to wild-type Tks5 was correlated to a large extent with increased Tks5 tyrosine phosphorylation (Fig. 2B). These data suggest that the PX and second SH3 domains of Tks5 may partially impede Tks5 tyrosine phosphorylation and Nck binding.

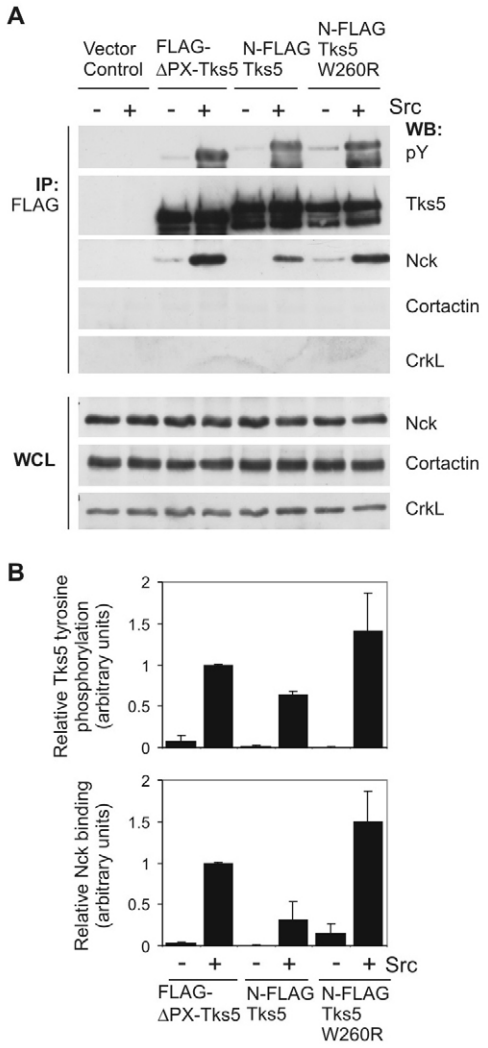

Fig. 2. Association of Nck with Tks5 is stimulated by Src but suppressed by the PX and second SH3 domains. (A) Co-immunoprecipitation and immunoblot analysis of extracts of 293T cells expressing N-terminal FLAG-tagged ΔPX-, full length or W260R Tks5 reveals that endogenous Nck1/2 (but not cortactin or CrkL) associate with all Tks5 variants in a Src-dependent manner. Nck binding is further enhanced by PX domain removal or mutation of the second SH3 domain. IP, immunoprecipitation, WCL, whole cell lysate. pY, phosphotyrosine. (B) Densitometry analysis of relative Tks5 tyrosine phosphorylation and Nck binding (normalized for Tks5 levels), reveals that ΔPX and W260R mutants are more phosphorylated and bind Nck more efficiently than N-FLAG-Tks5. Graphs show means + s.e.m. (n=2). Values for FLAG-ΔPX-Tks5 + Src were set arbitrarily at 1.

Src phosphorylates Tks5 at Y557 and promotes Nck association

Tks5 contains three candidate Src phosphorylation sites (Y552, Y557 and Y619; Fig. 3A) (Lock et al., 1998), two of which (Y552 and Y557) conform to consensus Nck SH2 domain binding sites {Y(*P*)DE[P/V/D]} (Songyang et al., 1993; Jones et al., 2006). Y557 and Y619 were confirmed to be Src phosphorylation sites in transfected Src-transformed NIH 3T3 cells (I.P., S.A.C. and P.L., unpublished data). To determine the contribution of these tyrosines to Nck binding, we generated FLAG-ΔPX-Tks5 constructs with Y552F, Y557F or Y619F substitutions, expressed them with or without Src in 293T cells and performed co-immunoprecipitation assays using a FLAG antibody. Endogenous Nck co-immunoprecipitated in a Src-inducible manner with wild-type and Y552F and Y619F mutant forms of FLAG-ΔPX-Tks5 but did not associate detectably with the Y557F mutant (Fig. 3B). Binding of Nck to full length C- and N-FLAG-Tks5 was also abolished by Y557F substitutions (Fig. 3C). Additionally, co-immunoprecipitation of Nck with N-FLAG-Tks5 could be competitively inhibited by pre-incubating lysates with a phosphopeptide containing the Nck binding site (Fig. 4A), but not by an unphosphorylated peptide of the same sequence, even at 15-fold higher concentrations (Fig. 3D). Together, these data show that Tks5 Y557 phosphorylation is critical for Nck binding.

Nck1 and Nck2 are closely related adaptor proteins containing three SH3 domains and a single SH2 domain (Fig. 3E). They share a broad and overlapping tissue distribution in the mouse embryo and appear to be functionally redundant in vivo, as mice deficient for Nck1 or Nck2 are viable, whereas those lacking both isoforms develop with severe abnormalities and die in utero (Bladt et al., 2003). These studies suggest that Nck1 and 2 may be largely interchangeable. To map the region(s) of Nck that facilitate binding to Tks5, HA-tagged human Nck1, Nck2 or Nck2 mutants with inactivated SH2 (Nck2 R311K) or SH3 domains (Nck2 W3K; Fig. 3E) were expressed with Src and wild-type or mutant forms of N-FLAG-Tks5 in 293T cells. Like endogenous Nck (Fig. 3C), HA-Nck1 and HA-Nck2 co-precipitated efficiently with wild-type Tks5 and were principally dependent for this interaction on the Y557 residue of Tks5 (Fig. 3F). However, we did observe some relatively weak binding of HA-Nck2 to Tks5 Y557F (Fig. 3F,G) although this interaction was not evident for Nck2 W3K, indicating that the SH3 domains of Nck2 mediate this association (Fig. 3F). Consistent with phosphorylated Y557 functioning as a docking site for the Nck SH2 domain, its inactivation markedly inhibited HA-Nck2 binding to wild-type N-FLAG-Tks5, although the much weaker (presumably SH3-mediated) interaction of Nck2 R311K with Tks5 Y557F remained (Fig. 3G; NB, the immunoblot is overexposed to demonstrate the interaction of HA-Nck2 with Tks5 Y557F. This exposure also reveals binding of endogenous Nck1/2, exclusively to wild-type Tks5).

To further probe the requirements of the Tks5-Nck interaction we performed an in vitro binding assay, incubating lysate from 293T cells coexpressing wild-type or mutant forms of Tks5 (plus or minus activated Src) with a GST-Nck1 SH2 domain fusion protein. Notably, the Nck1 and Nck2 SH2 domains show equivalent phosphopeptide binding specificities (Frese et al., 2006). SH2 binding proteins were precipitated on glutathione and analysed by immunoblotting with Tks5 and phosphotyrosine antibodies. Fig. 3H shows that wild-type, Y552F and Y619F variants were efficiently precipitated in a Src-inducible manner by the SH2 domain whereas, the Y557F mutants were not (Fig. 3H). Immunoblot analysis with a phosphotyrosine antibody provided an internal control for the integrity of the SH2 domain; endogenous 60 and 130 kDa proteins were efficiently precipitated from lysate of cells expressing the Tks5 Y557F mutants.

Lastly, we tested whether the Nck SH2 domain binds directly to Tks5 by using a far western (overlay) assay (Nollau and Mayer, 2001). Purified GST-Nck1 SH2 domain was incubated with the immunoblot shown in Fig. 3C and was found to bind specifically to immunoprecipitated C- and N-FLAG-Tks5 but did not bind the corresponding Y557F variants. Significantly, the relative levels of Nck SH2 domain bound to C- and N-FLAG-Tks5 in the overlay assay are in close agreement with the amounts of Nck co-

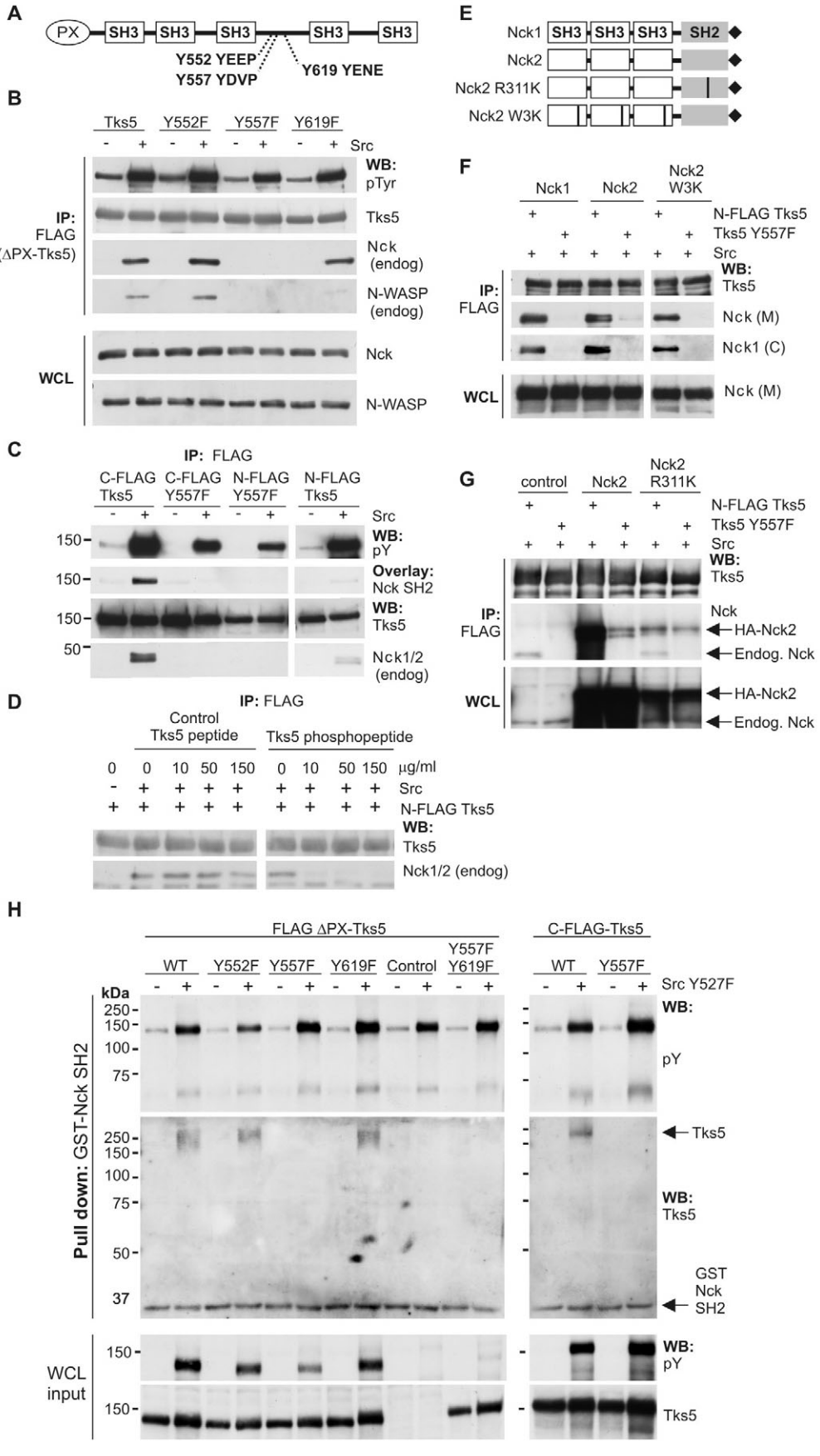

Fig. 3. Phosphorylation at Y557, but not Y552 or Y619, promotes a direct interaction between Tks5 and the Nck SH2 domain. (A) Diagram of Tks5 showing the location of candidate phosphorylation sites. (B). Immunoprecipitation analysis of extracts of 293T cells expressing FLAG-ΔPX-Tks5 or the indicated variants, identifies Y557 as a critical determinant of Src-induced Nck association. Re-probing for endogenous N-WASP shows that Y557 also enables N-WASP association, but is not sufficient in the Y619F mutant to permit maximal N-WASP binding. (C) Immunoprecipitation experiment showing requirement by full length Tks5 proteins for an intact Y557 residue for Nck co-immunoprecipitation in 293T cells. Overlay (far western) analysis with recombinant GST-Nck1 SH2 domain reveals that Nck binds the Y557 site directly. (D) Peptide competition experiment showing that incubation of 293T lysates with a Tks5 phosphopeptide based on the predicted Nck binding site of human Tks5 (Fig. 4A), but not its unphosphorylated counterpart, blocks Src-induced co-immunoprecipitation of endogenous Nck with FLAG-Tks5. (E) Schematic diagram of HA-Nck1, HA-Nck2 and Nck2 variants with inactivating point mutations in the SH2 (R311K) and all three SH3 domains (W3K). HA tag (diamond) and point mutations (vertical bars) are indicated. (F) Co-immunoprecipitation experiment showing that association of HA-Nck1 and HA-Nck2 with Tks5 in 293T cells relies primarily on Tks5 Y557; a weak Y557-independent interaction of Nck2 with Tks5 requires the Nck2 SH3 domains. Inexplicably, this interaction was not apparent with another antibody ('Nck1') which also recognises Nck2. C, antibody from Cell Signaling Technology; M, from Millipore. (G) Co-immunoprecipitation analysis showing that Y557-dependent, but not -independent association of HA-Nck2 with Tks5 requires an intact SH2 domain. (H) Pull down assay using recombinant GST Nck1 SH2 domain and extracts of 293T cells expressing the indicated proteins shows that Src-stimulated precipitation of Tks5 by the SH2 domain is Y557 dependent.

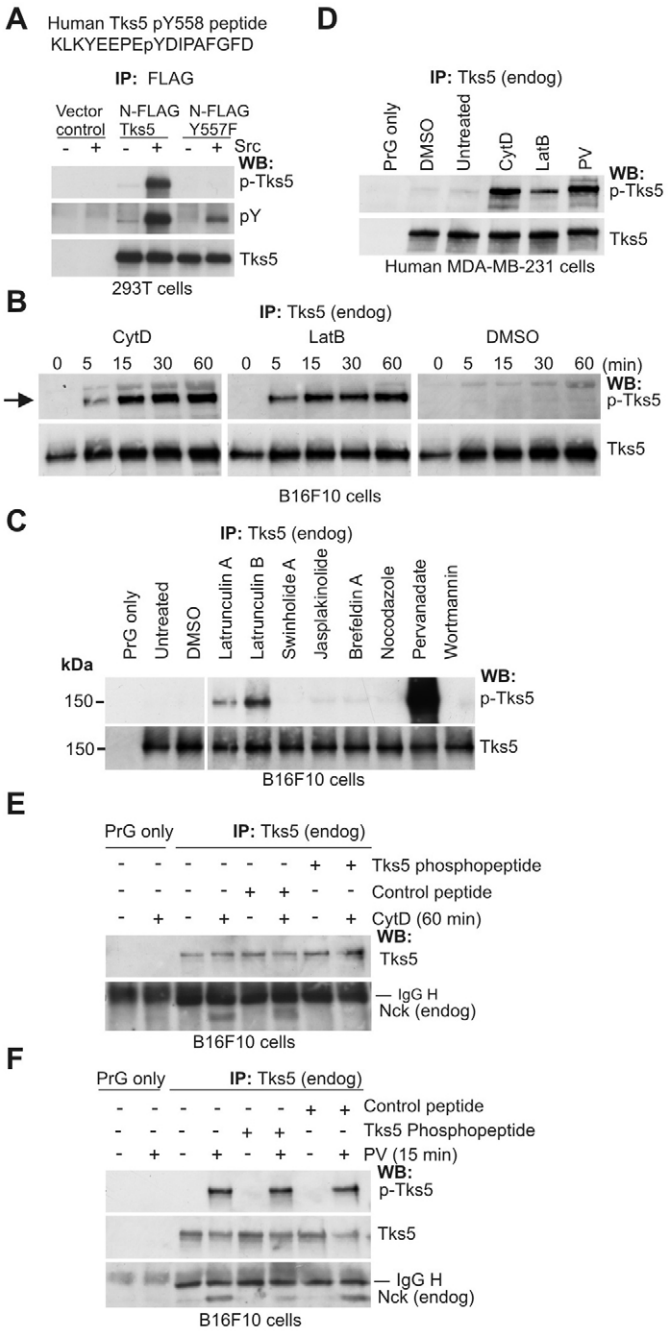

Fig. 4. Phosphorylation of endogenous Tks5 at Y557/8 and association with endogenous Nck are stimulated by inhibitors of actin polymerization and tyrosine phosphatases. (A) Tks5 phosphopeptide used to generate p-Tks5 antibody. Immunoprecipitation experiment showing specific recognition by affinity-purified p-Tks5 antibody of FLAG-Tks5 (but not Y557F) isolated from 293T cells coexpressing Src. (B) Time course experiment showing Y557-specific phosphorylation of immunoprecipitated endogenous Tks5 is induced in B16F10 cells with cytochalasin D (CytD) or latrunculin B (LatB) but not DMSO. (C,D) Immunoprecipitation experiments using (C) mouse B16F10 and (D) human MDA-MB-231 cells treated for 30 minutes with various inhibitors show that Tks5 Y557-specific (mouse) and Y558-specific (human) phosphorylation are boosted by cytochalasin D, latrunculin A and B and pervanadate. Concentrations used: latrunculin A (1 μM); latrunculin B (5 μM); swinholide A (0.1 μM); jasplakinolide (0.5 μM); brefeldin A (10 nM); nocodazole (5 μM); cytochalasin D (1 μM); wortmannin (0.1 μM); pervanadate (40 μM). Mouse and human Tks5 were immunoprecipitated with 6G1 or 2F4 antibodies, respectively. PrG, Protein G.
(E,F) Immunoprecipitation experiments using B16F10 cells grown for 3 hours on 0.1% gelatin and treated (+) or not treated (–) with cytochalasin D (1 μM, 1 hour, E) or pervanadate (PV, 40 mM, 15 minutes, F), show increased co-immunoprecipitation of endogenous Nck with endogenous Tks5 from lysates of the CytD- and PV-treated cells. Nck co-immunoprecipitation was strongly or partially inhibited by pre-incubation of cell lysates with Tks5 phosphopeptide compared with a control peptide (both 10 μg/ml).

immunoprecipitated in each case. Collectively, these data indicate that Nck associates directly with Tks5 and the primary determinants of this interaction are the Y557 phosphorylation site and the Nck1/2 SH2 domain.

Evidence that Src promotes a Tks5–Nck–N-WASP ternary complex

N-WASP is critical for podosome assembly in Src-transformed cells and EGF-induced invadopodia in mammary carcinoma cells (Mizutani et al., 2002; Yamaguchi et al., 2005; Co et al., 2007). Recently, N-WASP was identified as a Tks5 SH3-domain-binding protein and proposed to regulate Tks5-mediated actin assembly in podosomes (Oikawa et al., 2008). As Nck can also interact with N-WASP via its SH3 domains and can activate N-WASP to stimulate actin polymerization in vitro and in cells (Rohatgi et al., 2001; Rivera et al., 2004; Tehrani et al., 2007) we were interested to examine whether the interaction of N-WASP with Tks5 is affected by Nck binding. Reprobing the immunoblot shown in Fig. 3B revealed a Src-dependent interaction of endogenous N-WASP with FLAG-ΔPX-Tks5. This interaction was abolished by mutation of Y557, the Nck binding site, but intriguingly, was also partially reduced by mutation of Y619 without a noticeable effect on Nck binding. Although these experiments utilise a mutant form of Tks5 lacking the PX domain, this form of Tks5 contains all five SH3 domains. These data provide evidence that association of Tks5 with N-WASP is regulated by Y557 and Y619 phosphorylation and suggest that N-WASP could associate indirectly with Tks5 at least in part, via Nck.

Tks5 is phosphorylated at Y557/8 in vivo and associates with endogenous Nck

To assess whether Y557 and its counterpart in human Tks5 (Y558) are phosphorylation sites in vivo we raised an antibody against a 17 residue phosphopeptide based on human Tks5 (Fig. 4A). The human sequence differs from mouse Tks5 at the Y+2 position (V in mouse Tks5, I in human Tks5). The affinity-purified antibody, p-Tks5, was judged to be specific as it recognised immunoprecipitated N-FLAG-Tks5, but not the Y557F variant in lysates from Src-expressing 293T cells and was minimally reactive against Tks5 in the absence of Src co-expression (Fig. 4A). Furthermore, the antibody showed no reactivity towards another phosphorylated tyrosine in N-FLAG-Y557F detected with a general phosphotyrosine antibody.

Analysis of endogenous Tks5 Y557/8 phosphorylation in mouse B16F10 and human MDA-MB-231 cells revealed that this site is minimally phosphorylated in unstimulated cells (Fig. 4B-D). As Tks5 tyrosine phosphorylation is responsive to cell treatment with the actin polymerisation inhibitor cytochalasin D (Lock et al., 1998) we tested whether cytochalasin D or an unrelated actin polymerisation inhibitor, latrunculin B, affected Tks5 Y557/8-specific phosphorylation. Both inhibitors enhanced Tks5 Y557/8

phosphorylation in B16F10 and MDA-MB-231 cells compared with vehicle alone (Fig. 4B-D). By contrast, treatment of B16F10 cells with swinholide A, an F-actin severing agent, or jasplakinolide, which induces actin polymerisation, had little effect on Tks5 Y557 phosphorylation (Fig. 4C). Y557 phosphorylation was also unaffected by treatment of cells with brefeldin A, nocodazole or wortmannin. Perhaps not surprisingly, incubation of cells with pervanadate, to inhibit tyrosine phosphatases, strongly potentiated Tks5 Y557/8 phosphorylation (Fig. 4C,D). These data suggest that the Y557/8 residue is a phosphorylation site in vivo but imply that its phosphorylation is maintained at low steady state levels in cells by mechanisms, currently unknown, requiring the activities of tyrosine phosphatase(s) and/or actin polymerization.

We investigated the interaction of endogenous Tks5 and Nck in B16F10 melanoma cells. Cells were allowed to attach to gelatin-coated dishes for 3 hours to maximize recruitment of Tks5 to invadopodia puncta (supplementary material Fig. S1B; and data not shown) and then treated (or left untreated) with cytochalasin D or pervanadate. Cell lysates were then prepared and Tks5 immunoprecipitated. Endogenous Tks5-Nck complexes were barely detectable or were absent in untreated cells but could be immunoprecipitated from both cytochalasin D- and pervanadate-treated cells (Fig. 4E,F). Significantly, co-immunoprecipitation of Nck was selectively inhibited by the Tks5 phosphopeptide containing the Nck SH2 binding site but not by a control unphosphorylated peptide (Fig. 4E,F). These results confirm a specific association between endogenous Tks5 and Nck in cells, mediated primarily by the Nck SH2 domain and the Tks5 Y557 phosphorylation site.

Tks5 recruits Nck to invadopodia

Our results suggest that Nck could be recruited to invadopodia through a physical interaction with Tks5. We first examined the localization of Tks5-GFP and a red fluorescent protein (RFP)-Nck1 fusion protein in live Src-expressing B16F10 cells grown on Cascade Blue-labelled gelatin for 4 hours. Tks5-GFP and RFP-Nck1 were present in the cytoplasm of cells but were most highly concentrated in ventral puncta, many of which corresponded to functional invadopodia (Fig. 5A). By contrast, GFP or RFP alone did not localize specifically to ventral sites (not shown). In a separate experiment, B16F10 cells expressing active Src together with FLAG-Tks5 and HA-Nck1 were fixed then stained with Tks5 and HA antibodies (Fig. 5B). In these cells we could also detect strong colocalization of Tks5 and Nck in invadopodia. Interestingly, in some cells, Tks5-Nck puncta were also organized into large clusters or 'arrays' (Fig. 5B). To ascertain whether Y557 has a role in Nck targeting to invadopodia, we compared the localization of endogenous Nck in cells coexpressing active Src and wild-type or Y557F mutant forms of Tks5-GFP. Both Tks5-GFP proteins accumulated in numerous ventral puncta in the cells, indicating that Tks5 targeting to invadopodia does not require Y557. By contrast, the colocalization of endogenous Nck within Tks5-GFP-positive puncta appeared to be highly reliant on an intact Y557 residue (Fig. 5C). While some low level diffuse staining of endogenous Nck was observed in Tks5-Y557F-GFP puncta, this could potentially be due to interaction of Nck with endogenous (wild-type) Tks5. These data suggest that Tks5 Y557 phosphorylation signals Nck recruitment to invadopodia.

Tks5 requires Y557 for maximal activity and cooperates with Nck to promote matrix degradation

The functional role of Tks5 tyrosine phosphorylation was evaluated by comparing the area of gelatin degraded by B16F10 cells

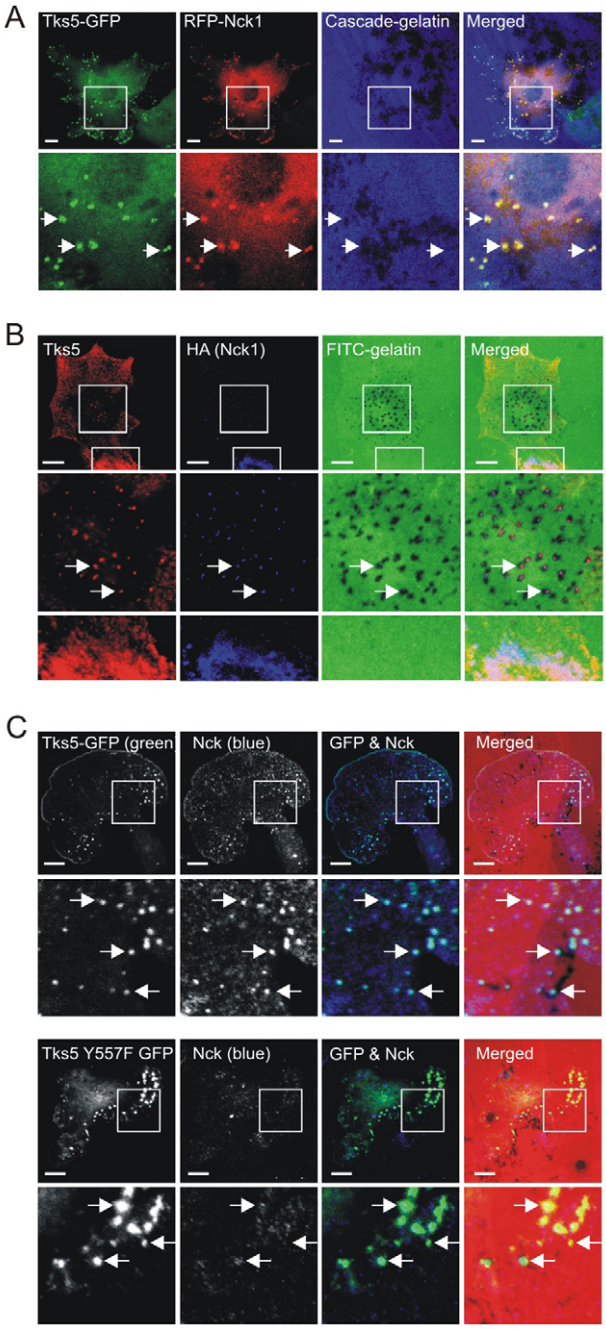

Fig. 5. Recruitment of endogenous Nck to invadopodia puncta is mediated by Tks5 Y557. (A) Confocal microscopy images showing colocalization of Tks5-GFP (green) and RFP-Nck1 (red) in a live Src-expressing B16F10 cell 4 hours after seeding onto Cascade Blue-labelled gelatin (blue). Boxed areas are enlarged in lower panels. Arrows indicate colocalization. (B) Confocal images of a B16F10 cell transfected with N-FLAG-Tks5, HA-Nck1 and Src, cultured for 4 hours on FITC-gelatin (green) and stained with Tks5 and HA antibodies shows Tks5 (red) and Nck (blue) colocalization in invadopodia (arrows) and in a large array with no underlying degradation. Middle and lower panels are enlargements of the areas indicated in the upper panels. (C) Confocal images of representative B16F10 cells coexpressing Src Y527F and Tks5-GFP (green, upper panels) or Tks5-Y557F-GFP (lower panels) and cultured for 4 hours on Rhodamine-gelatin (red). Staining for endogenous Nck using an 'Nck1' antibody that also detects Nck2 (see Fig. 3F) shows that Nck colocalizes tightly with Tks5-GFP puncta but shows limited colocalization with Tks5-Y557F-GFP sites. Arrows indicate the positions of three GFP-positive puncta in each cell. Scale bars: 10 μm.

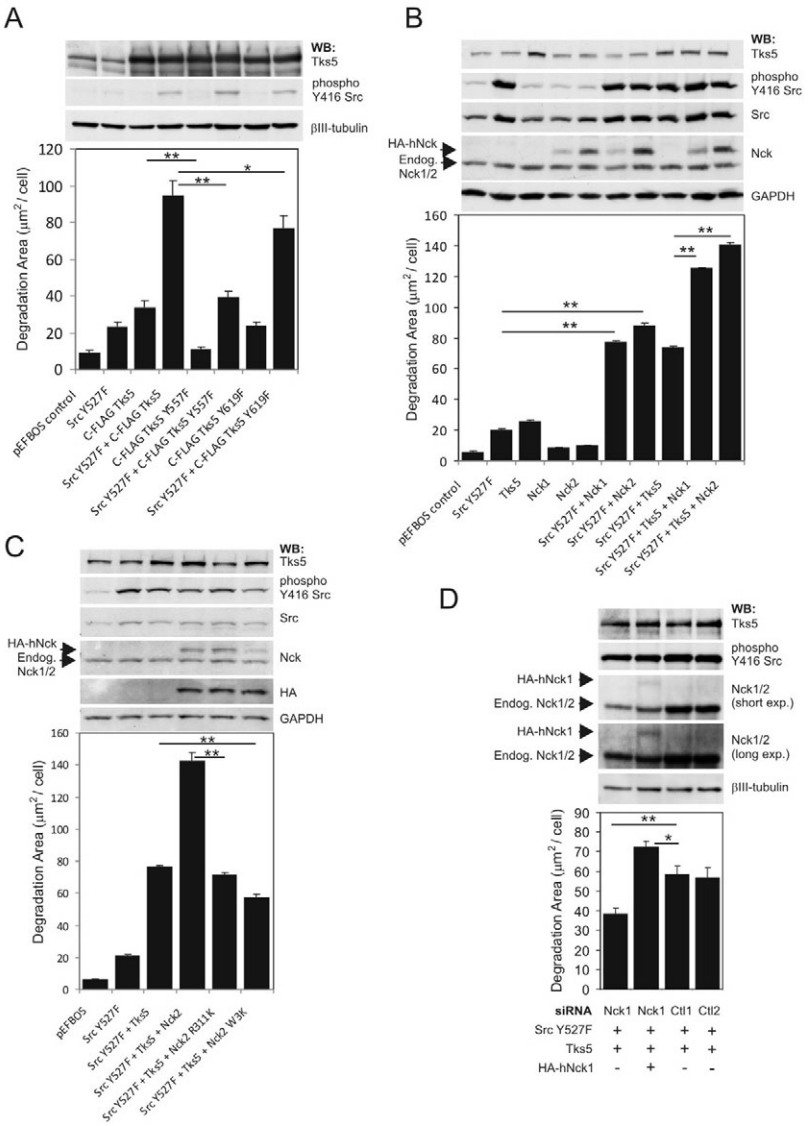

Fig. 6. Src, Tks5 and Nck cooperate to promote ECM degradation. (A-D) Quantification of FITC- or Rhodamine-gelatin degradation by B16F10 cells transiently expressing various wild-type and mutated Tks5, Nck and Src constructs, with the corresponding immunoblots showing expression of relevant proteins. Graphs indicate the mean degradation area/cell for each group + s.e.m. Representative confocal microscopy images are presented in supplementary material Fig. S3A-D. (A) Tks5 functional activity is dramatically reduced by mutation of Y557 with loss of activity evident in both Src Y527F-expressing and non-expressing cells. Mutation of Y619 results in a mild loss of activity, evident only in Src Y527F-expressing cells. n=20 fields, 465-644 cells (DAPI + nuclei)/group, two experiments; $^{**}P<0.01$, $^{*}P<0.05$ for the indicated pairs. (B) Nck1 and Nck2 cooperate with active Src and Tks5 to promote matrix degradation. n=10 fields, >160 cells/group; one experiment; $^{**}P<0.01$. (C) Functional cooperation between Nck2, Src and Tks5 is abolished by inactivating mutations in the SH2 or SH3 domains. n=10 fields, >150 cells/group; $^{**}P<0.01$ for indicated comparisons. (D) Partial depletion of endogenous Nck levels with Nck1 siRNA reduces Src Y527F and Tks5-induced matrix degradation by B16F10 cells. Re-expression of human HA-Nck1 reversed this effect albeit without apparent restoration of endogenous Nck1 levels. Ctl1 and Clt2 are unlabelled and fluoroscein-labelled non-targeting control siRNAs, respectively. n=20 fields, 260-340 cells/group, two experiments; $^{**}P<0.01$, $^{*}P<0.05$ for indicated pairs.

transiently expressing wild-type C-FLAG-Tks5 or the tyrosine substitution mutants, Y557F and Y619F, either alone or together with activated Src. The capacity of C-FLAG-Tks5 to stimulate matrix degradation, both in Src Y527F-expressing and non-expressing cells, was dramatically suppressed by mutating Y557 (Fig. 6A; supplementary material Fig. S3A). This mutation did not appear to fully disable Tks5 (or result in a dominant negative mutant) however, as Src-induced matrix degradation was still enhanced slightly by overexpressed Tks5 Y557F. Intriguingly, the ability of wild-type C-FLAG-Tks5 to cooperate with Src Y527F in promoting matrix degradation was also partially dependent on Y619, although we found no significant reduction in matrix degradation by cells expressing only Tks5 Y619F compared with those overexpressing wild-type Tks5. These results suggest that both Y557 and Y619, to different degrees, contribute to the functional activation of Tks5 and may explain why the individual Y mutants do not exhibit dominant negative activity. An analysis of Tks5 single and tandem tyrosine mutants on a Tks5 null (or depleted) background will be important to more precisely evaluate the relative contributions of these residues.

We next examined the consequences of Nck1 or Nck2 overexpression in B16F10 cells on FITC-gelatin degradation. Overexpression of Nck1 or Nck2 alone had minimal impact on basal matrix degradation (Fig. 6B; supplementary material Fig. S3B). By contrast, Src-induced proteolysis was profoundly increased by Nck1 or Nck2 (to similar levels as observed for Tks5). Maximal induction of matrix degradation was observed for cells coexpressing active Src, Tks5 and Nck2 (Fig. 6B; supplementary material Fig. S3B). Significantly, however, functional cooperation of Nck2 with Src Y527F and Tks5 was highly dependent on a functional Nck2 SH2 domain and all three SH3 domains (Fig. 6C; supplementary material Fig. S3C). Indeed, the Nck2 SH3 domain mutant, Nck2 W3K, partially suppressed Src Y527F and Tks5-induced matrix degradation in a dominant inhibitory manner (Fig. 6C; supplementary material Fig. S3C).

To assess the requirement for Nck in Tks5-dependent matrix degradation, RNAi was employed to deplete endogenous Nck1/2 in B16F10 cells expressing active Src and N-FLAG-Tks5. Although the Nck2 siRNA had no effect on endogenous Nck levels in our hands (not shown), treatment of cells with Nck1 siRNA reduced

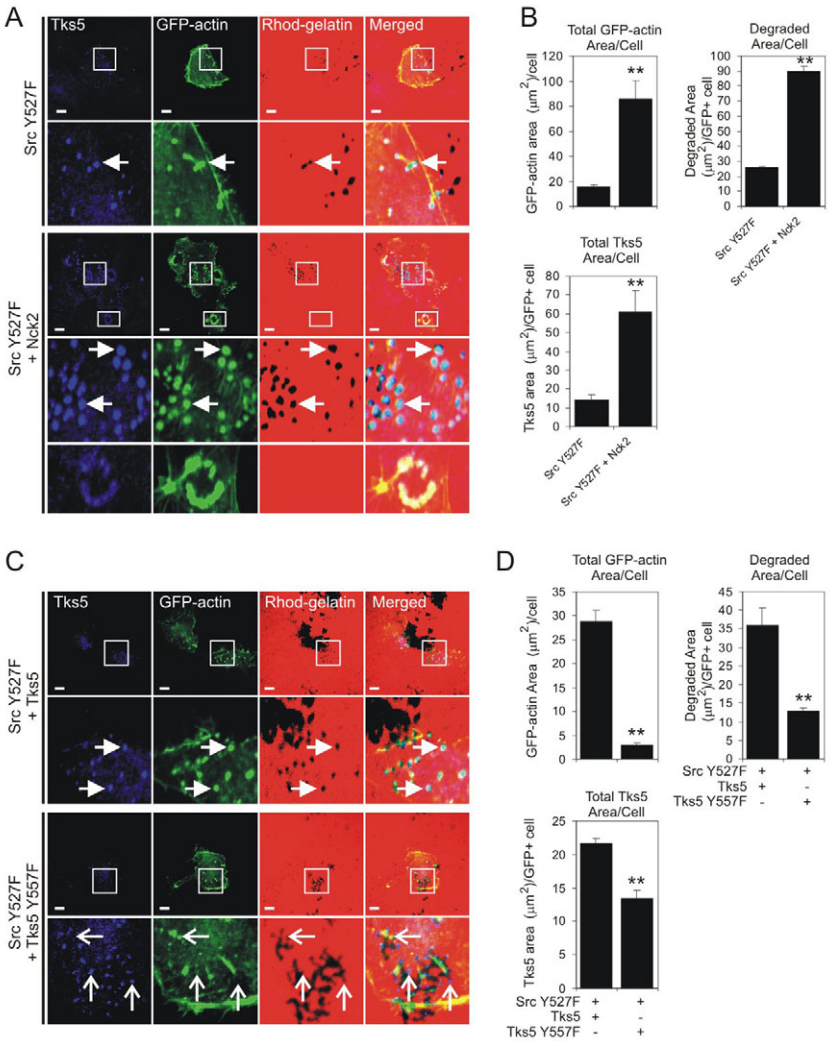

Fig. 7. Accumulation of ventral actin puncta in Src Y527F-expressing B16F10 cells is enhanced by Nck2 overexpression but is inefficient in cells expressing Tks5 Y557F. (A) Confocal microscopy images of B16F10 cells expressing Src Y527F and GFP-actin (green), plus or minus HA-Nck2, 4 hours after seeding on Rhodamine-gelatin (red). Expression of HA-Nck2 resulted in larger and more numerous GFP-actin and Tks5 puncta (blue), and increased matrix degradation. Boxed areas are enlarged in lower panels. Localization of GFP-actin and Tks5 in invadopodia (arrows) and in an ordered rosette-like array not associated with matrix degradation (rectangle) are indicated. Scale bars: 10 μm. (B) Quantification of the ventral area occupied by GFP-actin and Tks5 and the degradation area/cell in cells shown in A reveals that all three parameters are increased by Nck2 overexpression. Graphs show means + s.e.m. (n=10 cells/group). $^{**}P<0.01$ compared with Src Y527F control. (C) Images of B16F10 cells coexpressing Src Y527F, GFP-actin (green) and N-FLAG-Tks5 or N-FLAG-Y557F (blue) showing colocalization of Tks5 and GFP-actin in ventral puncta in cells expressing wild-type Tks5 (upper panels, arrows) but reduced correspondence of Tks5 and GFP-actin puncta in Tks5-Y557F-expressing cells (lower panels, open arrows). (D) Quantification of the GFP-actin and Tks5 areas and matrix degradation area for the cells in C, showing that all three parameters are reduced in Tks5 Y557F cells. Graphs show means + s.e.m. n=5 cells/group. $^{**}P<0.01$ compared with Src Y527F + wild-type N-FLAG-Tks5.

total Nck levels in B16F10 cells by approximately 55% when compared with cells treated with either of two different control non-targeting siRNAs, Ctl1 and Ctl2 (Fig. 6D; supplementary material Fig. S3D; and data not shown. NB, Nck antibody detects both Nck1 and Nck2). The fluoroscein-conjugated Ctl2 siRNA was used to estimate the average siRNA transfection efficiency at 61%. Treatment with the Nck1 siRNA resulted in a partial but significant reduction in matrix degradation by cells and this effect was overcome by coexpression of siRNA-resistant human HA-Nck1. Paradoxically, the relative levels of HA-Nck1 in cells appear to be too low to account for the observed phenotypic rescue; however, highly similar results were obtained in three separate experiments (Fig. 6D; and data not shown). One possible explanation is that the HA-epitope tag interferes with recognition of HA-Nck1 by the Nck antibody and underestimates its real levels. We conclude from the data presented in Fig. 6 that Src, Tks5 and Nck cooperate in B16F10 cells to stimulate matrix degradation.

Nck links Tks5 to invadopodial actin regulation

Nck adaptor proteins physically couple diverse mammalian and pathogen-encoded proteins to local actin regulation (Frischknecht et al., 1999; Gruenheid et al., 2001; Woodring et al., 2004; Jones et al., 2006; Verma et al., 2006). Current models propose that Nck adaptors are recruited to tyrosine phosphorylated target proteins via their SH2 domains, enabling Nck SH3 domain-associated molecules (e.g. N-WASP) to facilitate local actin regulation (Rohatgi et al., 2001; Campellone et al., 2004; Rivera et al., 2004). To determine if Nck has a role in invadopodial actin regulation, we monitored the distribution of GFP-actin in B16F10 cells coexpressing Src Y527F alone (control) or Src Y527F plus HA-Nck2. Cells were cultured for 4 hours on Rhodamine-labelled gelatin and counter-stained for endogenous Tks5 to enable functional invadopodia to be visualized. In Src Y527F-only cells, GFP-actin was detectable in three compartments; in cytoplasm, ventral puncta and in actin stress fibres (Fig. 7A). By contrast, in Nck2-overexpressing cells GFP-actin was mainly punctate in its localization and was reduced in the cytoplasm and fibres. In a subset of the Nck2-overexpressing cells GFP-actin puncta were also assembled into prominent semi-circular arrays. Measurements revealed three- and twofold increases in the number and area of individual GFP actin puncta in the Nck2-overexpressing cells compared with the control cells (data not shown). This translated to a more than fourfold increase in GFP-actin at the ventral membrane of the Nck2-overexpressing cells (Fig. 7B). We observed extensive colocalization of GFP-actin with endogenous Tks5 in both cell populations. However, Nck2 overexpression enhanced the size, number and combined area of Tks5 puncta, with these changes paralleling those of GFP-actin (Fig. 7B; and data not shown). Measurement of the degradation area per

GFP-actin-positive cell showed that the Nck2-overexpressing cells degraded over fourfold more gelatin than control Src Y527F-expressing cells. Collectively, these results show that Nck2 cooperates with Src and Tks5 to stimulate actin accumulation in invadopodia.

We next compared GFP-actin distribution in B16F10 cells expressing constitutively active Src and either N-FLAG-Tks5 or the Y557F mutant lacking the Nck binding site. Cells were cultured on Rhodamine-gelatin for 4 hours then fixed and stained with a Tks5 antibody to identify cells that clearly overexpressed Tks5. Although wild-type Tks5 colocalized prominently with GFP-actin, the Y557F mutant showed limited colocalization with GFP-actin (Fig. 7C, arrows, lower panels). Evaluation of the number, size and cumulative area of GFP-actin puncta showed that these parameters were markedly reduced in cells expressing Tks5 Y557F compared with those expressing wild-type Tks5 (Fig. 7D; and data not shown). By comparison, the size of Tks5 puncta was similar in wild-type and Y557F mutant-expressing cells (not shown) and the numbers and combined area of Tks5 puncta, although less in these cells, were not reduced to the same extent as GFP-actin. Consistent with our earlier results (Fig. 6A), cells expressing Src Y527F and Tks5 Y557F degraded the gelatin matrix less efficiently than those expressing Src Y527F and wild-type Tks5. Overall, these results suggest that Y557 couples Tks5 to actin regulation in invadopodia.

Clustering of the Tks5 linker region containing Y557 at the plasma membrane stimulates actin assembly

To determine if the inter-SH3 region of Tks5, containing the Nck docking site, is capable of directing actin regulation in cells, we adopted a receptor chimera strategy (Campellone et al., 2004; Rivera et al., 2004; Jones et al., 2006). Three receptor chimeras were constructed in which the CD16 extracellular and CD7 transmembrane domains were fused to GFP (control) or to the linker region of Tks5 containing the intact (or mutated) Nck binding site followed by GFP (supplementary material Fig. S4A). In this system, cross linking of receptors by incubation of cells with a CD16 antibody and a fluorescently labelled secondary antibody is used to manipulate (and visualize) receptor aggregation on the cell surface (supplementary material Fig. S4B). In control experiments we confirmed that incubation of B16F10 cells expressing the CD16/CD7-GFP chimera with cross-linking antibodies, but not secondary antibody alone, induced receptor clustering that could be detected by CD16 and GFP colocalization (supplementary material Fig. S4C). Furthermore, analysis of CD16/CD7-Tks5-GFP chimera phosphorylation with the p-Tks5 antibody showed that Y557 phosphorylation was strongly enhanced by receptor aggregation (supplementary material Fig. S4D).

We next evaluated the effect of receptor aggregation on the distribution of an RFP-Nck1 fusion protein. RFP-Nck1 was recruited to the clustered CD16/CD7-Tks5-GFP receptor at multiple sites at the cell periphery but did not colocalize with either the CD16/CD7-Y577F-GFP or CD16/CD7-GFP receptors (supplementary material Fig. S4E). To determine the impact of receptor clustering on actin regulation, CD16/CD7 receptor chimeras were expressed in B16F10 cells with HA-Nck2, cells were treated with cross linking antibodies, then fixed and stained with TRITC-phalloidin to visualize F-actin. Each of the receptor chimeras underwent extensive clustering in response to antibody treatment as indicated by colocalization of the anti-CD16 and GFP signals (Fig. 8). Strikingly, however, whereas the clustered CD16/CD7-Tks5-GFP receptors colocalized with numerous F-actin structures (white signal), the CD16/CD7-Y557F-GFP and the control CD16/CD7-GFP receptors did not. These data indicate the Nck binding region of Tks5 can mediate actin recruitment in the absence of the Tks5 SH3 domains.

Discussion

We describe a pathway used by invasive tumour cells to promote invadopodia and ECM proteolysis. Collectively our results and those of others suggest the following model (Fig. 9). Activation of Src, for example, in response to integrin-mediated adhesion to ECM

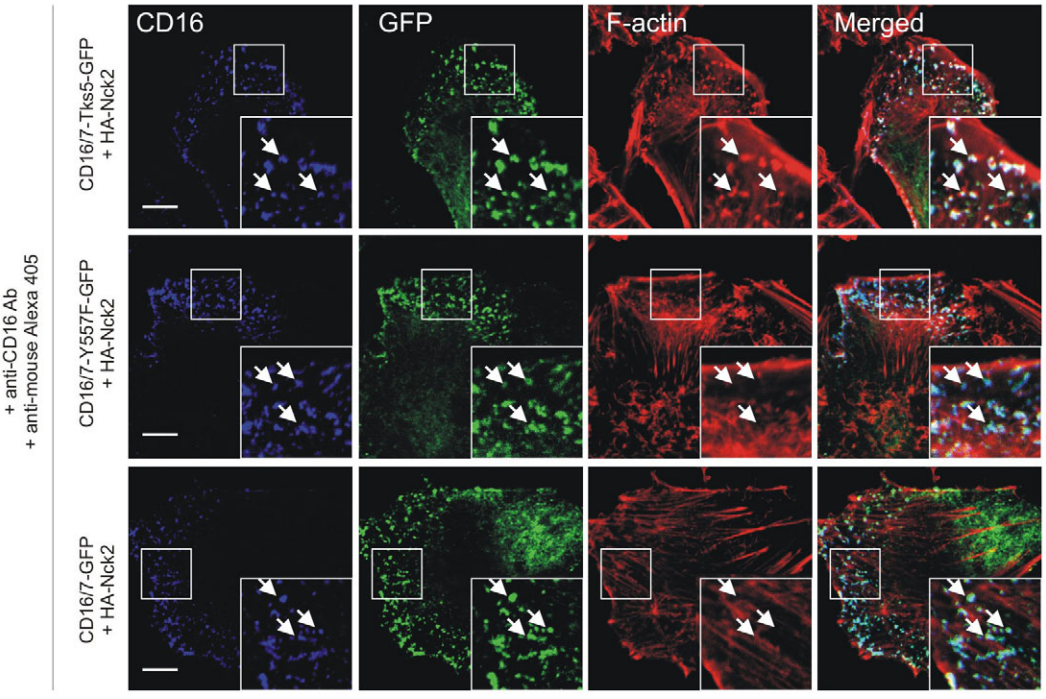

Fig. 8. Clustering of chimeric CD16/CD7 receptors containing the Tks5 inter-SH3 region encompassing Y557 promotes actin recruitment. Confocal images showing examples of B16F10 cells expressing CD16/CD7-Tks5-GFP, CD16/CD7-Y557F-GFP or control receptor chimeras (green) and HA-Nck2 after treatment with cross-linking antibodies (anti-CD16 plus Alexa Fluor 405 anti-mouse IgG; blue) and F-actin staining (red). Receptor clustering is induced on all cells (turquoise signal) but significant F-actin colocalization with receptors is only apparent in the cell expressing CD16/CD7-Tks5-GFP (white signal). Scale bars: 10 μm.

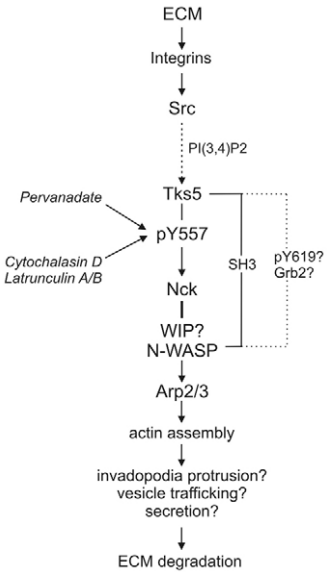

Fig. 9. Model: a Src-Tks5-Nck signalling pathway in invadopodia. Interaction of tumour cells with the ECM activates Src and PtdIns(3,4)P_2-dependent targeting of Tks5 to nascent invadopodia (Oikawa et al., 2008). Phosphorylation of Tks5 at Y557/8 promotes the recruitment of Nck adaptor proteins via their SH2 domains. Nck-associated N-WASP (possibly linked via the intermediate WIP) activates Arp2/3-mediated actin network assembly, potentially facilitating protrusive and/or trafficking events. How and whether these processes are linked to ECM degradation is not known. Tks5 can also associate with N-WASP via its SH3 domains (Oikawa et al., 2008) or possibly, via Y619 and Grb2. Inhibitors of tyrosine phosphatases and actin polymerization provoke Y557 phosphorylation and Nck association.

substrates (Mitra and Schlaepfer, 2006), promotes the phosphorylation of Tks5 at Y557/8 to generate a specific binding site for the SH2 domains of the Nck adaptor proteins. As Y557 was dispensable for Tks5-GFP localization in invadopodia, but important for Nck colocalization, we propose that Tks5 Y557 phosphorylation occurs in invadopodia and provides a signal for Nck recruitment to these sites. The initial targeting of Tks5 to invadopodia probably involves binding of its PX domain to membrane-localized PtdIns(3,4)P_2, as occurs in the initial phases of podosome assembly in Src-transformed fibroblasts (Oikawa et al., 2008; Symons, 2008). Once recruited to invadopodia, Nck proteins are postulated to regulate actin network assembly via Nck SH3 domain-associated proteins such as N-WASP and its key target, the Arp2/3 actin nucleation complex (Rohatgi et al., 2001; Rivera et al., 2004). Tks5-Nck-mediated actin assembly in invadopodia could potentially regulate protrusive or vesicular trafficking events in invadopodia. How local actin assembly promoted by Tks5-Nck complexes is linked to increased peri-cellular ECM degradation awaits further investigations, but presumably this requires increased focal expression of proteases such as MT1-MMP (Artym et al., 2006; Clark et al., 2007).

Recent evidence suggests that Tks5 can bind constitutively to N-WASP by all or a subset of its SH3 domains (Oikawa et al., 2008). In this manner, Tks5–N-WASP complexes could conceivably regulate actin nucleation in invadopodia without any requirement for Nck adaptors. Although our data are not directly comparable with those of Oikawa et al. (Oikawa et al., 2008), which showed that Tks5 and N-WASP interact equally in Src-transformed or untransformed 3T3 cells, we found that association of endogenous N-WASP with a FLAG-ΔPX-Tks5 construct lacking the PX domain (but replete with SH3 domains) was entirely Src dependent. Furthermore, binding of N-WASP was abolished by mutation of the Y557 phosphorylation site that mediates Nck binding or reduced (without affect on Nck binding) by mutation of Y619, another phosphorylation site. These two tyrosine residues lie in the linker region between the third and fourth SH3 domains and although mutating them would not be expected to affect SH3 domain integrity, their phosphorylation could perhaps effect conformational changes that expose Tks5 SH3 domains to permit N-WASP binding. An alternative possibility is that N-WASP association with Tks5 requires, in addition to Nck, another adaptor protein binding to pY619. The SH3-SH2-SH3 adaptor Grb2, identified in this work and by others, as a Tks5-interacting protein (Oikawa et al., 2008), is a strong candidate. Grb2 association with Tks5 is potentially phosphorylation dependent, being elevated in Src-transformed cells and inhibited by the Src kinase inhibitor PP2 (Oikawa et al., 2008). Although the binding site has not been mapped, it is noteworthy that Y619 lies within a Grb2 SH2 domain-binding motif [Y(*P*)xNx] (Songyang et al., 1994). Also, Grb2 SH3 domains can bind to N-WASP and promote N-WASP-dependent actin nucleation (Carlier et al., 2000; Rohatgi et al., 2001; Scaplehorn et al., 2002). Compellingly, evidence of functional cooperativity between Grb2 and Nck has also been reported in other model systems (Scaplehorn et al., 2002; Garg et al., 2007). For example, studies of actin-based motility of vaccinia virus (see also below) have shown that Grb2 and Nck are coordinately recruited to tandem phosphorylation sites in the viral A36R protein and cooperate to bind N-WASP and promote virus motility (Scaplehorn et al., 2002). Our finding that Y619 is necessary for maximal N-WASP binding by ΔPX-Tks5 and for maximal Tks5-mediated matrix degradation in Src-expressing B16F10 cells is intriguing in this context. The potential for Tks5 to form both Nck-dependent and -independent complexes with N-WASP (Fig. 9), perhaps during different stages of invadopodia genesis, remains an area for further investigations.

Our observation that inhibitors of tyrosine phosphatases and actin polymerization in cells enhanced Tks5 Y557 phosphorylation and association with Nck from low basal levels indicates that these events are tightly controlled. The effect of cytochalasin D is counter-intuitive, however, as Tks5 Y557/8 phosphorylation and Nck recruitment to invadopodia puncta seem to facilitate increased actin assembly. These results may reflect a negative feedback loop, dependent on actin polymerization, that down-modulates Tks5 phosphorylation and Nck binding. Indeed, actin polymerization inhibitors can trigger the activation of Src- or Abl-family kinases in some cells (Lock et al., 1998; Maher, 2000; Woodring et al., 2004). It seems unlikely that inhibition of actin polymerization is required for Nck recruitment to invadopodia since recruitment of endogenous Nck to Tks5-GFP puncta in B16F10 cells did not require pre-treatment of cells with cytochalasin D, but was dependent on Y557 and expression of active Src. Studies in monocytic-lineage cells indicate key roles for microtubules and associated molecular motors (e.g. kinesin KIF1C) in regulating the formation, location and dynamics of podosomes, including their assembly in osteoclasts into podosome belts (Linder, 2007; Gimona et al., 2008). Future experiments utilizing inhibitors/stabilisers of microtubule polymerization will assess the role of a functional microtubule network in Nck (and Tks5) localization in invadopodia. Possible roles of Arf-mediated vesicle trafficking and PI 3-kinase signalling in Nck recruitment to invadopodia will also be investigated.

The proposed role of Nck in invadopodia is consistent with its role as a key intermediate in localized actin assembly in a variety of physiological and pathological settings. For example, in kidney podocytes, Nck1 and 2 are recruited to specific docking sites in the cytoplasmic domain of the nephrin receptor and regulate the maintenance of actin-based cellular processes involved in glomerular filtration (Jones et al., 2006; Verma et al., 2006). Tyrosine phosphorylation of Dok1 by Abl kinase also induces Nck binding and is linked to the formation of filopodia during cell spreading (Woodring et al., 2004). In vaccinia-virus-infected cells, discussed briefly already, the A36R protein binds Nck (via Y112-*P*), recruiting WIP and N-WASP and triggering the assembly of Arp2/3-dependent F-actin 'comets' that promote motility of extracellular viral particles (Frischknecht et al., 1999). Grb2, recruited to a second phosphorylated residue, Y132-*P*, cooperates with Nck in this process (Scaplehorn et al., 2002). Another pathogen, enteropathogenic *E. coli* (EPEC), also exploits Nck-dependent actin regulation in host cells. The EPEC transmembrane protein Tir is phosphorylated and binds to endogenous Nck, and N-WASP associated with Nck promotes the formation of actin 'pedestals' at the plasma membrane (Gruenheid et al., 2001). Using a receptor-clustering approach similar to that developed previously (Campellone et al., 2004; Rivera et al., 2004; Jones et al., 2006; Verma et al., 2006), we confirmed that the Nck binding region of Tks5, excluding its SH3 domains, but not a Y557-mutated variant, can promote F-actin assembly in the presence of transiently expressed Nck2 in cells. Nck SH3 domains bind directly or indirectly to several proteins involved in actin polymerization including WIP and its binding partner N-WASP (Moreau et al., 2000; Rohatgi et al., 2001; Benesch et al., 2002). Moreover in cell-free assays, purified Nck cooperates with N-WASP, WIP, cortactin and Arp2/3 to stimulate actin polymerization (Rohatgi et al., 2001; Tehrani et al., 2007) providing compelling evidence that these proteins are critical components of a multi-subunit actin-regulatory complex. Consistent with our results, others found that Nck1 (along with N-WASP, WIP and Arp2/3) is critical for EGF-induced invadopodia formation in MTLn3 mammary carcinoma cells (Yamaguchi et al., 2005). It was unclear from this study how EGF receptor signalling targets Nck to invadopodia but it is interesting to speculate that Src and Tks5 are important intermediates in this pathway.

Materials and Methods

Antibodies and reagents

The following antibodies were used: anti-FLAG M2 agarose (Sigma), anti-Nck (06-288) and anti-cortactin (4F11; Millipore), anti-N-WASP, anti-CrkL, anti-GAPDH, anti-phosphotyrosine (P-Tyr-100), anti-phospho Src family (TyrY416), anti-HA tag (6E2), anti-Nck1 (Cell Signaling Technology), anti-Fish (Tks5; M-300, Santa Cruz Biotechnology Inc.) and anti-CD16 (Beckman Coulter). Anti-Tks5 (Tks5.2) and anti-Src (2-17) antibodies have been described previously (Lock et al., 1998). Tks5 monoclonal antibodies (6G1 and 2F4) were generated in mice by immunisation with a GST-Tks5 fusion protein containing the fourth SH3 domain of mouse Tks5. The phosphospecific p-Tks5 antibody was raised in rabbits at the WEHI Biotechnology Centre (Melbourne) by immunisation with a synthetic human phosphopeptide, KLKYEEPEY558(*P*)DIPAFGFD coupled to diphtheria toxin (Auspep). Antisera were affinity-purified by removal of antibodies binding to an immobilized unphosphorylated Tks5 peptide and collection of those binding the phosphopeptide immunogen. Alexa Fluor 405, 488 and 546 anti-mouse and anti-rabbit IgGs and Cascade Blue were from Invitrogen. DAPI, TRITC-phalloidin, Rhodamine B isothiocyanate, 300 Bloom gelatin, DMSO, cytochalasin D, brefeldin A, nocodazole, swinholide A, wortmannin, latrunculin A and B and sodium orthovanadate, were purchased from Sigma. Jasplakinolide was obtained from Merck Biosciences and FITC from MP Biomedicals.

Plasmids and siRNA

DNA constructs encoding Tks5 and ΔPX-Tks5 (lacking the PX domain) with N- and/or C-terminal FLAG tags were generated by PCR using mouse Tks5 DNA template (Lock et al., 1998) and pEFBOS FLAG vectors (I et al., 2004). The Tks5-GFP construct was generated by PCR on mouse Tks5 (minus stop codon) and insertion in the pEGFP-C1 vector (Clontech). Plasmids encoding C-terminal 3x HA-tagged human Nck1 and Nck2 were generated by RT-PCR from a human glioma cDNA library (kindly provided by Nathan Godde, Dept. of Surgery, University of Melbourne, Victoria, Australia) and insertion into pcDNA3 (Invitrogen). Constructs encoding CD16/CD7 receptor chimeras were generated as follows: CD16 extracellular and CD7 transmembrane sequences were amplified by PCR using a CD16.7 plasmid kindly provided by Brian Seed (Harvard Medical School). The CD16/CD7 sequence was inserted into pEGFP-C1 (to generate CD16/CD7-GFP) and the PCR-amplified Tks5 region encoding residues 506-835 (with/without the Y557F mutation; supplementary material Fig. S3) was inserted into this backbone. Tks5 phosphorylation site mutants (Y552F, Y557F and Y619F) and Nck2 point mutants (R311K and W3K) were generated with a QuickChange XL mutagenesis kit (Stratagene). All PCR-generated regions were sequenced (Australian Genome Research Facility Ltd) and confirmed to be error-free. The following siRNA duplexes were purchased from Santa Cruz Inc: mouse Tks5/Fish (sc-35377), mouse Nck1 (sc-40968) and non-targeting control (sc-37007). Fluoroscein-conjugated control siRNA was from New England Biolabs.

Cell culture and transfection

Murine melanoma B16F10, human glioma D270, D54, D566, LN18 and mouse glioma SMA560 cells were gifts from Ulrike Novak (Dept of Surgery, University of Melbourne, Victoria, Australia). Human breast carcinoma MDA-MB-231, MDA-MB-435 and T47D cells and human melanoma MEL007, ME4405 and 624.38 cells were kindly provided by Phil Darcy (Peter McCallum Institute, Victoria, Australia). Rat C6 glioma and human U118MG, U251MG and U373MG glioma cells were obtained from ATCC. Cells were cultured as described previously (I et al., 2004). For DNA transfections, 1×10^6 (B16F10, MDA-MB-231) or 2×10^6 (293T) cells were seeded in 6 cm dishes and the following day transfected with 1 μg total DNA using Effectene Transfection Reagent (Qiagen). For siRNA transfections, 5×10^5 B16F10 cells/well were seeded in 12-well plates and cells transfected the next day with 50 nM siRNA (with or without 1 μg plasmid DNA). Cells were incubated for 16-18 hours (DNA) or 40-42 hours (siRNA) before matrix degradation and invadopodia assays were performing.

Identification of Tks5-interacting proteins

Plasmids encoding Src and FLAG-Tks5 proteins (supplementary material Fig. S2A) were co-transfected into subconfluent cultures of 293T cells in 60×15 cm dishes. 24 hours later, cells were washed with a solution of TBS, vanadate and 2 mM DTT and solubilized in lysis buffer (1% Triton X-100, 10% glycerol, 150 mM NaCl, 20 mM Tris pH 7.5, 2 mM EDTA, 10 μg/ml aprotinin, 10 μg/ml leupeptin and 1 mM PMSF). Clarified cell lysates were passed twice through columns of FLAG-M2 antibody beads (Sigma) as described previously (Verhagen et al., 2000). Following extensive washing, FLAG-Tks5 and associated proteins were eluted with 3× FLAG peptide (Sigma), the eluate concentrated by ultrafiltration using an Amicon ultrafiltration unit (10 kDa cut-off) and proteins separated by SDS-PAGE on 12% long (22 cm) gels (Hoefer). Proteins were visualised by staining the gels with Sypro Ruby (Invitrogen), and Phast-Blue Coomassie (Pharmacia). Protein bands were excised, digested in situ with trypsin and analysed by tandem mass spectrometry (Verhagen et al., 2000). The mass spectrometry and peptide sequence analysis was performed at the Joint ProteomicS Facility (JPSF), Melbourne.

Immunofluorescence

Gelatin was labelled with FITC or Rhodamine, applied to glass coverslips (25 mm diameter, 0.17±0.01 mm thickness; Menzel) and fixed with glutaraldehyde as described previously (Bowden et al., 2001). Cells (1×10^5) were seeded onto the coverslips in 6-well plates and incubated for 4 hours (to visualize invadopodia) or 24 hours (to assess cumulative matrix degradation). Cells were fixed in 4% paraformaldehyde in PBS for 15 minutes, washed with PBS then permeabilized in 0.2% Triton X-100 in PBS for 5 minutes. Washed cells were incubated with primary antibodies in 2% BSA in TBS containing 0.1% Tween 20 at RT for 1 hour. Cells were then washed and incubated with Alexa Fluor-conjugated anti-IgGs (Invitrogen) or stained for F-actin with TRITC-Phalloidin (Sigma) for 1 hour at room temperature. Following three further washes with PBS, coverslips were mounted on microscope slides with Vecta-Shield (Vector Laboratories). For detection of nuclei, DAPI (5 μg/ml) was included in the first of the final PBS washes.

Imaging and quantification of matrix degradation and puncta assays

Confocal microscopy images were acquired using a Nikon TE2000-E inverted microscope with Plan Apochromat VC ×60.0 and ×100 oil immersion, 1.40 NA, objectives. The microscope was linked to a Nikon C1 confocal system (equipped with 405, 488 and 532 nm lasers) and EZ-C1 acquisition software. Images were saved in Nikon ids format and converted using the Nikon EZ-C1 FreeViewer program to TIFF files for image analysis using ImageJ (v1.38) software (NIH). Threshold and region tools were used to define total regions of matrix degradation in a given field (fluorescence-negative areas) and the area of degradation computed using the particle counter function. Values obtained in pixels were converted to μm^2 and normalized with respect to the number of cells (DAPI-positive nuclei) in the field. Ten or more

fields of at least 150 cells/group were analysed and data expressed as degradation area (μm^2)/cell (mean ± s.e.m.). For the 4-hour matrix degradation assay, only fields with Tks5-GFP or GFP-expressing cells (n=10) were analysed. Results were expressed accordingly as degradation area (μm^2)/GFP-positive cell. For puncta determinations, the ImageJ region tool was used to trace the outline of all ventral puncta in a given cell and areas computed as above in 10 cells. Total GFP-actin (or Tks5) puncta area/cell was calculated by summing the values for each punctum in the cell.

Statistics

For analysis of four or more groups a global ANOVA analysis was performed followed by post-hoc Tukey-Kramer analysis. Experiments with two or three comparison groups were analysed using an unpaired t-test. Differences were considered significant if $P<0.05$.

Chimeric CD16/CD7-Tks5 receptor experiments

CD16/CD7-GFP receptor constructs were transiently expressed in B16F10 cells growing on coverslips. Medium was removed 24 hours after transfection and receptor clustering was induced by incubation of cells with anti-CD16 antibody (1 μg/ml) and/or Alexa Fluor 405 anti-mouse IgG (1:1,000) for various times at room temperature (Verma et al., 2006).

We thank Stephen Cody for confocal microscopy advice and training, Darren Seals for protocols to prepare labelled gelatin coverslips, Brian Seed, Ulrike Novak, Nathan Godde and Phil Darcy for plasmids and cell lines. This work was supported by grants from the NHMRC (Australia), the National Cancer Institute of the USA (NIH) and the John T. Reid Charitable Trusts. Deposited in PMC for release after 12 months.

References

Abram, C. L., Seals, D. F., Pass, I., Salinsky, D., Maurer, L., Roth, T. M. and Courtneidge, S. A. (2003). The adaptor protein fish associates with members of the ADAMs family and localizes to podosomes of Src-transformed cells. *J. Biol. Chem.* **278**, 16844-16851.

Ago, T., Kuribayashi, F., Hiroaki, H., Takeya, R., Ito, T., Kohda, D. and Sumimoto, H. (2003). Phosphorylation of p47phox directs phox homology domain from SH3 domain toward phosphoinositides, leading to phagocyte NADPH oxidase activation. *Proc. Natl. Acad. Sci. USA* **100**, 4474-4479.

Alexander, N. R., Branch, K. M., Parekh, A., Clark, E. S., Iwueke, I. C., Guelcher, S. A. and Weaver, A. M. (2008). Extracellular matrix rigidity promotes invadopodia activity. *Curr. Biol.* **18**, 1295-1299.

Artym, V. V., Zhang, Y., Seillier-Moiseiwitsch, F., Yamada, K. M. and Mueller, S. C. (2006). Dynamic interactions of cortactin and membrane type 1 matrix metalloproteinase at invadopodia: defining the stages of invadopodia formation and function. *Cancer Res.* **66**, 3034-3043.

Ayala, I., Baldassarre, M., Giacchetti, G., Caldieri, G., Tete, S., Luini, A. and Buccione, R. (2008). Multiple regulatory inputs converge on cortactin to control invadopodia biogenesis and extracellular matrix degradation. *J. Cell Sci.* **121**, 369-378.

Badowski, C., Pawlak, G., Grichine, A., Chabadel, A., Oddou, C., Jurdic, P., Pfaff, M., Albiges-Rizo, C. and Block, M. R. (2008). Paxillin phosphorylation controls invadopodia/podosomes spatiotemporal organization. *Mol. Biol. Cell* **19**, 633-645.

Baldassarre, M., Pompeo, A., Beznoussenko, G., Castaldi, C., Cortellino, S., McNiven, M. A., Luini, A. and Buccione, R. (2003). Dynamin participates in focal extracellular matrix degradation by invasive cells. *Mol. Biol. Cell* **14**, 1074-1084.

Basbaum, C. B. and Werb, Z. (1996). Focalized proteolysis: spatial and temporal regulation of extracellular matrix degradation at the cell surface. *Curr. Opin. Cell Biol.* **8**, 731-738.

Benesch, S., Lommel, S., Steffen, A., Stradal, T. E., Scaplehorn, N., Way, M., Wehland, J. and Rottner, K. (2002). Phosphatidylinositol 4,5-biphosphate (PIP2)-induced vesicle movement depends on N-WASP and involves Nck, WIP, and Grb2. *J. Biol. Chem.* **277**, 37771-37776.

Bharti, S., Inoue, H., Bharti, K., Hirsch, D. S., Nie, Z., Yoon, H. Y., Artym, V., Yamada, K. M., Mueller, S. C., Barr, V. A. et al. (2007). Src-dependent phosphorylation of ASAP1 regulates podosomes. *Mol. Cell. Biol.* **27**, 8271-8283.

Bladt, F., Aippersbach, E., Gelkop, S., Strasser, G. A., Nash, P., Tafuri, A., Gertler, F. B. and Pawson, T. (2003). The murine Nck SH2/SH3 adaptors are important for the development of mesoderm-derived embryonic structures and for regulating the cellular actin network. *Mol. Cell. Biol.* **23**, 4586-4597.

Bowden, E. T., Barth, M., Thomas, D., Glazer, R. I. and Mueller, S. C. (1999). An invasion-related complex of cortactin, paxillin and PKCmu associates with invadopodia at sites of extracellular matrix degradation. *Oncogene* **18**, 4440-4449.

Bowden, E. T., Coopman, P. J. and Mueller, S. C. (2001). Invadopodia: unique methods for measurement of extracellular matrix degradation *in vitro*. *Methods Cell Biol.* **63**, 613-627.

Campellone, K. G., Rankin, S., Pawson, T., Kirschner, M. W., Tipper, D. J. and Leong, J. M. (2004). Clustering of Nck by a 12-residue Tir phosphopeptide is sufficient to trigger localized actin assembly. *J. Cell Biol.* **164**, 407-416.

Carlier, M. F., Nioche, P., Broutin-L'Hermite, I., Boujemaa, R., Le Clainche, C., Egile, C., Garbay, C., Ducruix, A., Sansonetti, P. and Pantaloni, D. (2000). GRB2 links signaling to actin assembly by enhancing interaction of neural Wiskott-Aldrich syndrome protein (N-WASp) with actin-related protein (ARP2/3) complex. *J. Biol. Chem.* **275**, 21946-21952.

Chen, W. T., Olden, K., Bernard, B. A. and Chu, F. F. (1984). Expression of transformation-associated protease(s) that degrade fibronectin at cell contact sites. *J. Cell Biol.* **98**, 1546-1555.

Chuang, Y. Y., Tran, N. L., Rusk, N., Nakada, M., Berens, M. E. and Symons, M. (2004). Role of synaptojanin 2 in glioma cell migration and invasion. *Cancer Res.* **64**, 8271-8275.

Clark, E. S., Whigham, A. S., Yarbrough, W. G. and Weaver, A. M. (2007). Cortactin is an essential regulator of matrix metalloproteinase secretion and extracellular matrix degradation in invadopodia. *Cancer Res.* **67**, 4227-4235.

Co, C., Wong, D. T., Gierke, S., Chang, V. and Taunton, J. (2007). Mechanism of actin network attachment to moving membranes: barbed end capture by N-WASP WH2 domains. *Cell* **128**, 901-913.

Condeelis, J. and Segall, J. E. (2003). Intravital imaging of cell movement in tumours. *Nat. Rev. Cancer* **3**, 921-930.

Frese, S., Schubert, W. D., Findeis, A. C., Marquardt, T., Roske, Y. S., Stradal, T. E. and Heinz, D. W. (2006). The phosphotyrosine peptide binding specificity of Nck1 and Nck2 Src homology 2 domains. *J. Biol. Chem.* **281**, 18236-18245.

Friedl, P. and Wolf, K. (2003). Tumour-cell invasion and migration: diversity and escape mechanisms. *Nat. Rev. Cancer* **3**, 362-374.

Friedl, P. and Wolf, K. (2008). Tube travel: the role of proteases in individual and collective cancer cell invasion. *Cancer Res.* **68**, 7247-7249.

Frischknecht, F., Moreau, V., Rottger, S., Gonfloni, S., Reckmann, I., Superti-Furga, G. and Way, M. (1999). Actin-based motility of vaccinia virus mimics receptor tyrosine kinase signalling. *Nature* **401**, 926-929.

Garg, P., Verma, R., Nihalani, D., Johnstone, D. B. and Holzman, L. B. (2007). Neph1 cooperates with nephrin to transduce a signal that induces actin polymerization. *Mol. Cell. Biol.* **27**, 8698-8712.

Gimona, M., Buccione, R., Courtneidge, S. A. and Linder, S. (2008). Assembly and biological role of podosomes and invadopodia. *Curr. Opin. Cell Biol.* **20**, 235-241.

Groemping, Y., Lapouge, K., Smerdon, S. J. and Rittinger, K. (2003). Molecular basis of phosphorylation-induced activation of the NADPH oxidase. *Cell* **113**, 343-355.

Gruenheid, S., DeVinney, R., Bladt, F., Goosney, D., Gelkop, S., Gish, G. D., Pawson, T. and Finlay, B. B. (2001). Enteropathogenic E. coli Tir binds Nck to initiate actin pedestal formation in host cells. *Nat. Cell Biol.* **3**, 856-859.

Hashimoto, S., Onodera, Y., Hashimoto, A., Tanaka, M., Hamaguchi, M., Yamada, A. and Sabe, H. (2004). Requirement for Arf6 in breast cancer invasive activities. *Proc. Natl. Acad. Sci. USA* **101**, 6647-6652.

I, S. T., Nie, Z., Stewart, A., Najdovska, M., Hall, N. E., He, H., Randazzo, P. A. and Lock, P. (2004). ARAP3 is transiently tyrosine phosphorylated in cells attaching to fibronectin and inhibits cell spreading in a RhoGAP-dependent manner. *J. Cell Sci.* **117**, 6071-6084.

Jones, N., Blasutig, I. M., Eremina, V., Ruston, J. M., Bladt, F., Li, H., Huang, H., Larose, L., Li, S. S., Takano, T. et al. (2006). Nck adaptor proteins link nephrin to the actin cytoskeleton of kidney podocytes. *Nature* **440**, 818-823.

Karathanassis, D., Stahelin, R. V., Bravo, J., Perisic, O., Pacold, C. M., Cho, W. and Williams, R. L. (2002). Binding of the PX domain of p47(phox) to phosphatidylinositol 3,4-bisphosphate and phosphatidic acid is masked by an intramolecular interaction. *EMBO J.* **21**, 5057-5068.

Linder, S. (2007). The matrix corroded: podosomes and invadopodia in extracellular matrix degradation. *Trends Cell Biol.* **17**, 107-117.

Lock, P., Abram, C. L., Gibson, T. and Courtneidge, S. A. (1998). A new method for isolating tyrosine kinase substrates used to identify fish, an SH3 and PX domain-containing protein, and Src substrate. *EMBO J.* **17**, 4346-4357.

Maher, P. A. (2000). Disruption of cell-substrate adhesion activates the protein tyrosine kinase pp60(c-src). *Exp. Cell Res.* **260**, 189-198.

Mitra, S. K. and Schlaepfer, D. D. (2006). Integrin-regulated FAK-Src signaling in normal and cancer cells. *Curr. Opin. Cell Biol.* **18**, 516-523.

Mizutani, K., Miki, H., He, H., Maruta, H. and Takenawa, T. (2002). Essential role of neural Wiskott-Aldrich syndrome protein in podosome formation and degradation of extracellular matrix in src-transformed fibroblasts. *Cancer Res.* **62**, 669-674.

Moreau, V., Frischknecht, F., Reckmann, I., Vincentelli, R., Rabut, G., Stewart, D. and Way, M. (2000). A complex of N-WASP and WIP integrates signalling cascades that lead to actin polymerization. *Nat. Cell Biol.* **2**, 441-448.

Nollau, P. and Mayer, B. J. (2001). Profiling the global tyrosine phosphorylation state by Src homology 2 domain binding. *Proc. Natl. Acad. Sci. USA* **98**, 13531-13536.

Oikawa, T., Itoh, T. and Takenawa, T. (2008). Sequential signals toward podosome formation in NIH-src cells. *J. Cell Biol.* **182**, 157-169.

Onodera, Y., Hashimoto, S., Hashimoto, A., Morishige, M., Mazaki, Y., Yamada, A., Ogawa, E., Adachi, M., Sakurai, T., Manabe, T. et al. (2005). Expression of AMAP1, an ArfGAP, provides novel targets to inhibit breast cancer invasive activities. *EMBO J.* **24**, 963-973.

Rivera, G. M., Briceno, C. A., Takeshima, F., Snapper, S. B. and Mayer, B. J. (2004). Inducible clustering of membrane-targeted SH3 domains of the adaptor protein Nck triggers localized actin polymerization. *Curr. Biol.* **14**, 11-22.

Rohatgi, R., Nollau, P., Ho, H. Y., Kirschner, M. W. and Mayer, B. J. (2001). Nck and phosphatidylinositol 4,5-bisphosphate synergistically activate actin polymerization through the N-WASP-Arp2/3 pathway. *J. Biol. Chem.* **276**, 26448-26452.

Scaplehorn, N., Holmstrom, A., Moreau, V., Frischknecht, F., Reckmann, I. and Way, M. (2002). Grb2 and Nck act cooperatively to promote actin-based motility of vaccinia virus. *Curr. Biol.* **12**, 740-745.

Seals, D. F., Azucena, E. F., Jr, Pass, I., Tesfay, L., Gordon, R., Woodrow, M., Resau, J. H. and Courtneidge, S. A. (2005). The adaptor protein Tks5/Fish is required for podosome formation and function, and for the protease-driven invasion of cancer cells. *Cancer Cell* **7**, 155-165.

Journal of Cell Science

Songyang, Z., Shoelson, S. E., Chaudhuri, M., Gish, G., Pawson, T., Haser, W. G., King, F., Roberts, T., Ratnofsky, S., Lechleider, R. J. et al. (1993). SH2 domains recognize specific phosphopeptide sequences. *Cell* **72**, 767-778.

Songyang, Z., Shoelson, S. E., McGlade, J., Olivier, P., Pawson, T., Bustelo, X. R., Barbacid, M., Sabe, H., Hanafusa, H., Yi, T. et al. (1994). Specific motifs recognized by the SH2 domains of Csk, 3BP2, fps/fes, GRB-2, HCP, SHC, Syk, and Vav. *Mol. Cell. Biol.* **14**, 2777-2785.

Symons, M. (2008). Cell biology: watching the first steps of podosome formation. *Curr. Biol.* **18**, R925-R927.

Tague, S. E., Muralidharan, V. and D'Souza-Schorey, C. (2004). ADP-ribosylation factor 6 regulates tumor cell invasion through the activation of the MEK/ERK signaling pathway. *Proc. Natl. Acad. Sci. USA* **101**, 9671-9676.

Tehrani, S., Tomasevic, N., Weed, S., Sakowicz, R. and Cooper, J. A. (2007). Src phosphorylation of cortactin enhances actin assembly. *Proc. Natl. Acad. Sci. USA* **104**, 11933-11938.

Thompson, O., Kleino, I., Crimaldi, L., Gimona, M., Saksela, K. and Winder, S. J. (2008). Dystroglycan, Tks5 and Src mediated assembly of podosomes in myoblasts. *PLoS ONE* **3**, e3638.

Verhagen, A. M., Ekert, P. G., Pakusch, M., Silke, J., Connolly, L. M., Reid, G. E., Moritz, R. L., Simpson, R. J. and Vaux, D. L. (2000). Identification of DIABLO, a mammalian protein that promotes apoptosis by binding to and antagonizing IAP proteins. *Cell* **102**, 43-53.

Verma, R., Kovari, I., Soofi, A., Nihalani, D., Patrie, K. and Holzman, L. B. (2006). Nephrin ectodomain engagement results in Src kinase activation, nephrin phosphorylation, Nck recruitment, and actin polymerization. *J. Clin. Invest.* **116**, 1346-1359.

Weaver, A. M. (2006). Invadopodia: specialized cell structures for cancer invasion. *Clin. Exp. Metastasis* **23**, 97-105.

Woodring, P. J., Meisenhelder, J., Johnson, S. A., Zhou, G. L., Field, J., Shah, K., Bladt, F., Pawson, T., Niki, M., Pandolfi, P. P. et al. (2004). c-Abl phosphorylates Dok1 to promote filopodia during cell spreading. *J. Cell Biol.* **165**, 493-503.

Yamaguchi, H., Lorenz, M., Kempiak, S., Sarmiento, C., Coniglio, S., Symons, M., Segall, J., Eddy, R., Miki, H., Takenawa, T. et al. (2005). Molecular mechanisms of invadopodium formation: the role of the N-WASP-Arp2/3 complex pathway and cofilin. *J. Cell Biol.* **168**, 441-452.